JES Bulletin, 3(1):86-92, Jan – 2025

Open Access, Peer Reviewed, Research Journal

Print & Online available on https://jesbulletin.in

Research Article

Investigation of Structural, Optical and Antimicrobial Properties of Pristine and Ni-Doped ZnO Nanoparticles

Shaikh Mohd. Waseem [1,*], *Shaikh Ifrah Fatema* [1], *Mazahar Ahmad Farooqui* [2]

[1]*Department* [1]*Department of Physics, Maulana Azad College of Art, Science & Commerce, Aurangabad, India*
[2]*Department of Chemistry, Maulana Azad College of Art, Science & Commerce, Aurangabad, India*

**Corresponding Author: skwaseemphysics@gamil.com*

ARTICLE INFO

Received: 10/02/2024
Revised: 15/03/2024
Accepted: 01/04/2024

KEYWORDS

ZnO, Ni-doped ZnO, sol-gel synthesis, bandgap energy, antimicrobial activity,

ABSTRACT

The sol-gel method synthesized the pristine and Ni-doped ZnO nanoparticles and characterized them in their physical attributes and antimicrobial activity. The hexagonal wurtzite structure of the samples was confirmed by the X-ray diffraction (XRD) analysis with the successful incorporation of the Ni ions and an increase in the crystallite size of 31.46 nm of zinc oxide (ZnO) to 34.28 nm of Ni-doped ZnO. Structural changes obtained on FTIR spectroscopy, such as Zn-O bond vibrations due to Ni dopant in the regular bonding sites of pure ZnO lattice. SEM analysis with EDS confirmed elemental composition and suggested reduced aggregation and improved dispersion for Ni-doped ZnO. The UV-Vis spectroscopy confirmed that the bandgap decreased from 2.9 eV (ZnO) to 2.6 eV (ZnO: Ni), thus better visible light absorption. For the antimicrobial activity against E. coli and S. aureus, the inhibition zones were significantly higher for the Ni-doped ZnO than ZnO.

1 Introduction

Zinc oxide (ZnO) is a remarkably advantageous material in nanotechnology because of its exceptional optical, physical and chemical qualities. As a direct wide-bandgap semiconductor with an energy bandgap of around 3.37 eV and a high exciton binding energy of 60 meV at room temperature, ZnO discovers use in optoelectronics, photocatalysis, spintronics and gas sensing. Its nontoxic character, chemical stability and cost-effectiveness further improve its suitability for environmental and industrial applications. However, despite such outstanding properties, pure ZnO has specific constraints that limit its broader practicality. For example, its wide bandgap restricts absorption to the ultraviolet (UV) region, diminishing its efficacy in visible-light-driven processes. Additionally, pure ZnO lacks intrinsic magnetic properties, which are crucial for spintronic applications [1].

To address these constraints, doping ZnO with transition metals like nickel (Ni) has developed as an effective strategy. Ni doping introduces localized defect states in the ZnO lattice, considerably modifying its electronic structure. These alterations narrow the bandgap, allowing Ni-doped ZnO to absorb visible light and boosting its photocatalytic effectiveness. Moreover, the integration of Ni ions induces room-temperature ferromagnetism, opening new This study synthesizes and evaluates pristine and Ni-doped ZnO nanoparticles, emphasizing their antimicrobial activity against possibilities for multifunctional uses such as spintronics and magnetic storage devices [2].

Beyond optical and magnetic improvements, Ni doping enhances ZnO antimicrobial qualities, a critical attribute for healthcare and environmental applications. The presence of Ni in the ZnO matrix heightens the generation of reactive oxygen species (ROS) like hydroxyl radicals (•OH), superoxide anions (O_2^-•), and hydrogen peroxide (H_2O_2). These ROS disturb bacterial membranes, harm cellular parts and eventually lead to cell death. The electrostatic interactions between the positively charged Ni-doped ZnO nanoparticles and negatively charged bacterial surfaces magnify its antibacterial efficacy [3].

The synthesis of Ni-doped ZnO nanoparticles has been extensively investigated using various methods, including sol-gel, chemical and green synthesis approaches. These methods permit control over particle size, morphology and crystallinity, which are crucial for optimizing functional properties. Structural analyses confirm that Ni-doped ZnO retains its hexagonal wurtzite structure, even at higher doping levels, with localized distortions influencing defect density and crystallite size. These modifications are pivotal in enhancing antimicrobial activity and optical and electronic properties [4].

Escherichia coli (E. coli) and Staphylococcus aureus (S. aureus). By leveraging the benefits of Ni doping, this work aims to

demonstrate the potential of Ni-doped ZnO as an advanced material for environmental remediation, healthcare and multifunctional device applications.

2. Experimental

The nanoparticles of pure ZnO and Ni-doped ZnO were synthesized through the sol-gel method. Zinc acetate dihydrate ($Zn(CH_3COO)_2 \cdot 2H_2O$) and nickel acetate tetrahydrate ($Ni(CH_3COO)_2 \cdot 4H_2O$) were provided as zinc precursor and nickel doping source, respectively. Citric acid was used as a chelator, and deionized water as a solvent. All the chemicals used were of analytical grade and used without further purifications. A 0.5 M zinc acetate dihydrate solution was prepared in deionized water for the pure ZnO nanoparticles and then stirred at room temperature until dissolved. Then, citric acid was incorporated into this solution as a chelating agent in a 1:3 molar ratio. The mixture was further mixed and heated to 80 °C until an optically clear gel appeared. The resulting gel was dried overnight at 100 °C to eliminate remaining water molecules, and it was then calcined at 500 °C for 3 h to acquire pure ZnO nanoparticles.

Ni-doped ZnO NPs were prepared using a similar method, using nickel acetate tetrahydrate as a precursor to the dopant. To obtain a doping concentration of 5 wt. Preparation of nickel acetate in different percentages in 0.5 M zinc acetate solution. Citric acid was added in the same mole ratio of 1:3, and the solution was stirred and heated at 80°C until a homogeneous gel formed. The gel was then dried overnight at 100 °C in an oven and calcined at 500 °C for three h to obtain Ni-doped ZnO nanoparticles.

3. Results and Discussion

3.1 XRD Analysis

Figure 1 shows the X-ray diffraction (XRD) patterns of pure and Ni-doped ZnO nanoparticles. The diffraction peaks of prominent features for both samples are located at the hexagonal wurtzite structure of ZnO (JCPDS Card No. 36–1451) [5]. These characteristic peaks correspond to the (100), (002), (101), (102), (110), (103), (200), (112) and (201) planes, and appear at 2θ values of 31.7°, 34.4°, 36.2°, 47.5°, 56.6°, 62.8°, 66.3°, 67.9°, and 69.1° respectively. The presence of these diffraction peaks reveals the phase purity of the synthesized samples.

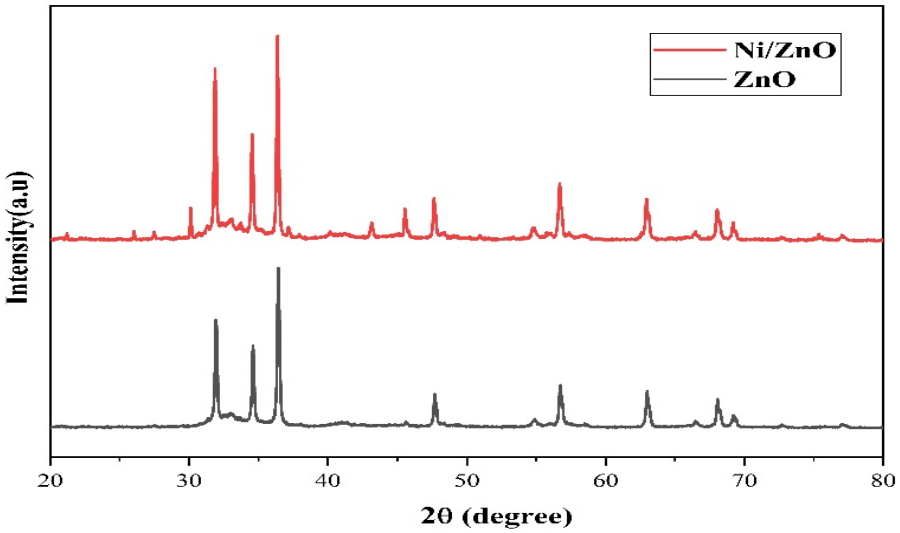

The Ni-doped ZnO nanoparticles did not show any extra peaks associated with nickel oxide (NiO) or other impurity phases and confirmed the incorporation of Ni. Ions into the ZnO lattice. This indicates the substitution of Ni^{2+} ions instead of Zn^{2+} ions in the wurtzite lattice but without affecting the crystalline structure. The position of peaks was slightly changed for the Ni-doped sample compared to the pure ZnO. Such changes are ascribed to the ionic radii difference between Zn^{2+} (0.74 Å) and Ni^{2+} (0.69 Å), which causes lattice strain and structural distortions. The crystallite size of the nanoparticles was calculated using the Debye-Scherrer formula [5] $D = K\lambda/\beta\cos\theta$, Where D is the crystallite size, K is shape factor (0.9), λ is X-ray wavelength (1.5406 Å), β is full width at half maximum (FWHM) of the diffraction peak in radians, and θ is Bragg angle. By calculation, the crystallite size of pure ZnO was found to be 31.46 nm and 34.28 nm for the Ni-doped ZnO. The crystallite size increase with Ni doping results from the structural rearrangement due to Ni^{2+} ions substitution, which affects the overall crystal growth process [6]. The broadening of diffraction peaks of Ni-doped sample over pure ZnO provides strong evidence for the incorporation of Ni into the lattice of wurtzite-type ZnO because a certain amount of lattice strain and defect density are introduced into the material when foreign ions enter the lattice of a crystal [7]. The structural changes are anticipated to affect the required material properties, such as optical and electronic ones. The XRD results confirm the formation of pure and Ni-doped ZnO nanoparticles with hexagonal

wurtzite structure and indicate that Ni doping can alter the structure while preserving the phase purity.

3.2 FTIR Analysis

Figure 2 shows the FTIR spectra of pure ZnO and Ni-doped ZnO nanoparticles. The representative peaks of the functional groups and bonds were visualized through both spectra of the samples. The peaks verify ZnO has formed, and Ni is doped in the ZnO lattice [8], [9].

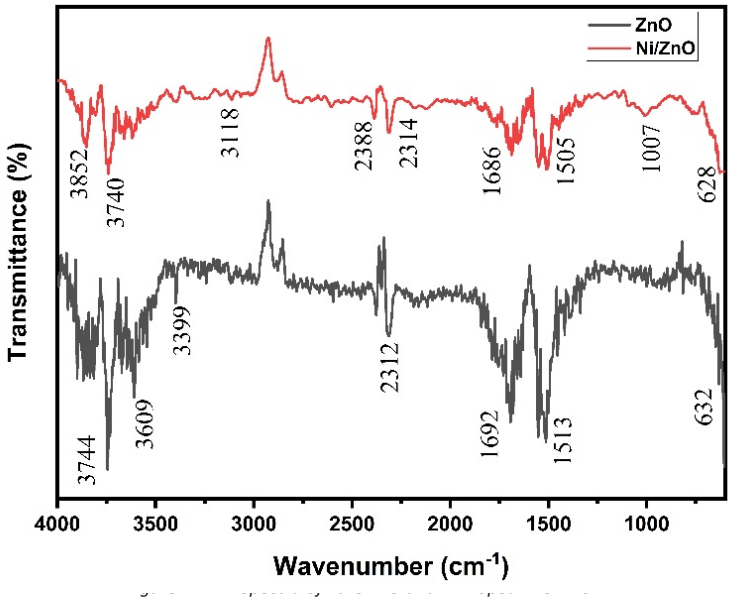

the spectrum of pure ZnO, the broad absorption band observed in the region of 3399–3744 cm^{-1} is assigned to O–H stretching vibrations of the adsorbed water molecules or hydroxyl groups on the surface of the nanoparticles [10]. Ni-doped ZnO also shows this feature but at a lower intensity, confirming a lower degree of surface adsorption or a doping-induced structural change [7]. The bands in the range 1505–1692 cm^{-1} are associated with bending vibrations of absorbed water molecules (that is, absorbed water vapour), thus verifying the presence of moisture for both pure and Ni-doped ZnO samples. These differences in the peak shifts for Ni-doped ZnO are due to changes in the local environment due to Ni incorporation.

The absorption band at 628–632 cm^{-1} is different, attributed to the stretching mode of Zn–O, a spectral characteristic of the ZnO wurtzite structure. This peak is slightly shifted and broadened in Ni-doped ZnO, which confirms the successful Ni doping process and may also suggest that the Ni–O bonds are formed. Localized distortions due to the presence of Ni in the lattice may result in the vibrational mode being slightly changed. The heights of the minor peaks seen in both spectra in the 2300–2400 cm^{-1} correspond to vibrations of atmospheric CO_2. They are generally observed in FTIR spectra, which do not influence the structural properties of the samples. The peaks of the Ni-doped ZnO spectrum at 1007–1505 cm^{-1} are relatively enhanced concerning pure ZnO. These peaks can be related to other vibrational modes excited by the incorporation of Ni atoms, changed to a chemical environment and memorized by defects.

The FTIR analysis confirms the formation of pure and Ni-doped ZnO nanoparticles showing Zn–O stretching vibration. The shifts and changes of peak intensity for Ni-doped ZnO demonstrate that we could find a window for incorporating Ni ions into the ZnO lattice with significant structural modifications. This is coherent with the broader findings of the XRD analysis that reinforce the stability of the structural features of the doped samples [11].

3.3 Scanning Electron Microscopy (SEM) Analysis

The different surface morphology of the pure ZnO and Ni-doped ZnO nanoparticles is well observed from the SEM image micrograph, which indicates the effect of Ni doping on the ZnO. Due to the high surface energy property of the pure ZnO nanoparticles, the particles influence strong particle-particle interactions, resulting in agglomerated clusters of extremely irregularly shaped sustainable ZnO nanoparticles. The nanoparticles seem to agglomerate into compact beaded formations with a relatively homogenous, albeit less-defined structure. The Ni-doped ZnO nanoparticles show a significant reduction in the degree of aggregation, forming a somewhat defined structure that is relatively uniformly dispersed. The average particle size of Ni-doped ZnO is larger than pure ZnO, which agrees with the crystallite size (as examined in XRD). The substitution of Zn^{2+} ions by Ni^{2+} ions inhibits the growth process during growth, causing larger sizes and better dispersion. Such morphological changes due to Ni doping may be crucial to the optical and electronic properties of the material [12].

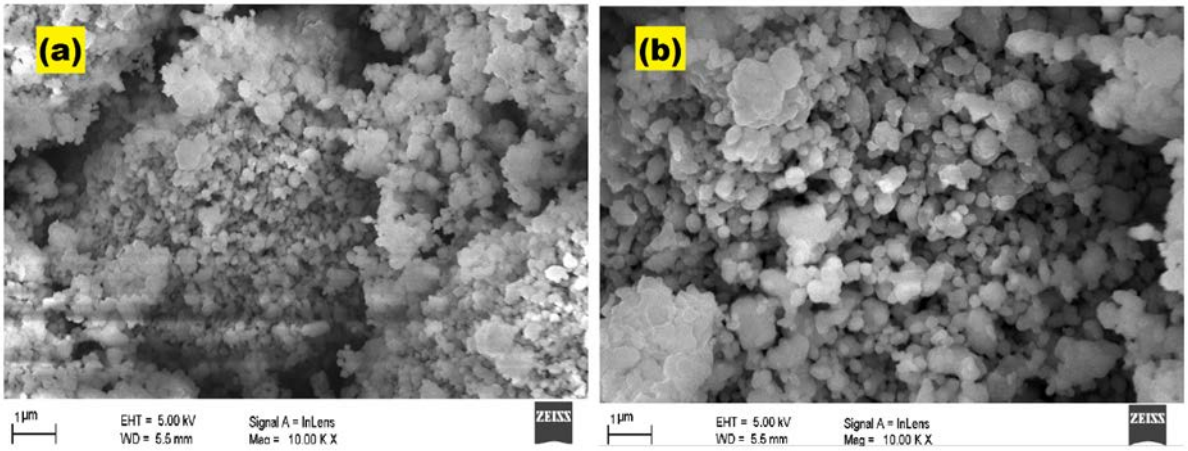

Figure 3: SEM Micrographs of (a)Pure ZnO and (b)Ni-Doped ZnO Nanoparticles.

3.4 Energy Dispersive X-Ray Spectroscopy (EDS) Analysis

Energy Dispersive X-ray Spectroscopy (EDS) provided insight into the elemental structure and verified that nickel had been incorporated into the ZnO crystal framework as intended. As one would predict, examining the EDS spectra for pure ZnO and Ni-doped ZnO nanoparticles revealed the signature elements of zinc and oxygen in both samples. However, extra peaks representing nickel were observed for the doped ZnO, confirming that nickel had been added to the ZnO matrix through the doping process. Analysis of the pure ZnO specimen showed the zinc-to-oxygen ratio was close to the stoichiometric proportion, suggesting high purity and no impurities present.

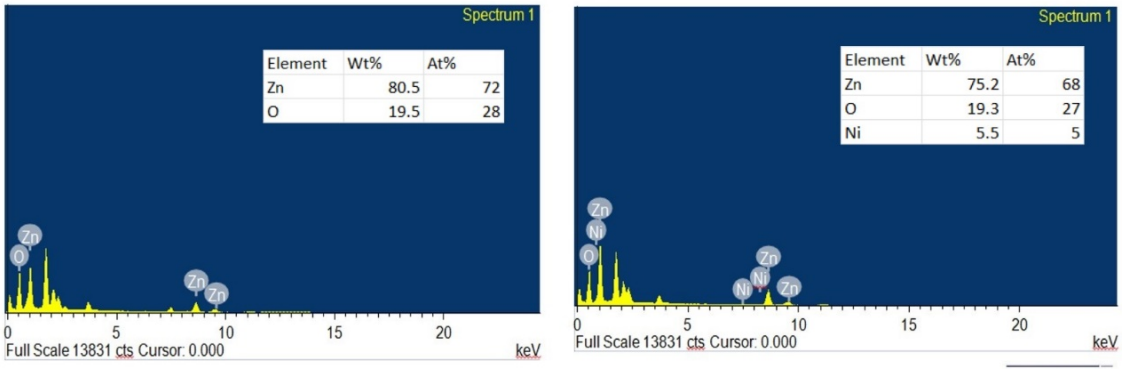

Figure 4: EDS Spectra of Pure ZnO and Ni-Doped ZnO Nanoparticles.

In the case of nickel-doped zinc oxide, the detected nickel content was consistent with the anticipated doping concentration, further validating the successful substitution of zinc ions by nickel ions. The lack of peaks corresponding to additional elements or impurities in both samples' spectra signifies the synthesized nanoparticles' high purity. The EDS analysis buttresses the structural and morphological findings, demonstrating the efficient synthesis of pure and nickel-doped zinc oxide nanoparticles with regulated elemental composition. These conclusions substantiate the synthesis method and emphasize the part of nickel doping in customizing the qualities of zinc oxide. Intriguingly, the controlled introduction of nickel permitted modifications to properties like conductivity, enabling innovative pathways for applications that demand optimized performance. The consistent and homogenous distribution of dopants was crucial for reproducible results, achieved through carefully monitored temperature parameters during synthesis[13].

3.5 UV-Vis Spectroscopy Analysis

The UV-Vis spectra of pure and Ni-doped ZnO nanoparticles were used to study the optical properties presented as Tauc plots in Figure 5. ZnO is typically known for its high absorption in the region above the UV range. However, the absorption spectra can visualize the massive modification in its optical behavior due to Ni doping. The absorption edge of pure ZnO was seen at 284 nm, which corresponds to a bandgap energy of 2.9 eV, which was determined from the Tauc plot according to the relation [14] $(\alpha h\nu)^2 = A(h\nu - Eg)$, where α is the absorption coefficient, hν is the photon energy, A is a constant, and Egis the optical band gap. Identifying the bandgap energy: The bandgap energy was established from linear extrapolation of the linear portion of the Tauc plot to the energy axis (hν).

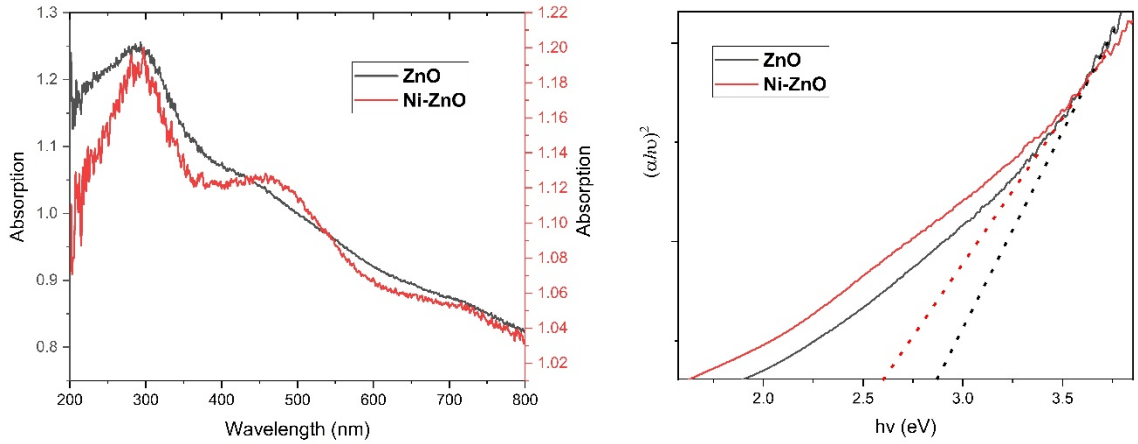

Figure 5: UV-Vis Absorption Spectra and Tauc Plots for Bandgap

The absorption edge redshifted toward a lower energy bandgap of 2.6 eV for Ni-doped ZnO. Such bandgap narrowing has also been attributed to introducing the local energy states in the band structure by substituting Ni^{2+} ions into the lattice of ZnO by forming an intermediate band structure. These states reduce the effective bandgap and increase the power absorption of the material from visible light. Compared to pure ZnO, the Tauc plot for Ni-doped ZnO shows less pronounced characteristics [[15], and a slight broadening can be seen, which is an indication of defect states and lattice distortions caused by doping [16]. This ultimately leads to structural changes responsible for the redshift in the absorption edge, enhancing visible light absorption. The UV-Vis results indicate that ZnO shows different optical behaviour when doped with Ni, lowering the bandgap energy and expanding the light absorption range.

Antimicrobial Activity

The disc diffusion method assessed the antimicrobial activity of ZnO and Ni-doped ZnO nanoparticles against Gram-negative Escherichia coli (E. coli) and Gram-positive Staphylococcus aureus (S. aureus). Overnight bacterial cultures were inoculated onto nutrient agar plates and adjusted to the 0.5 McFarland turbidity standard (1.5×10^8 CFU/mL around). Discs impregnated with 10 mg/mL ZnO and Ni-doped ZnO suspensions were placed on the plates, with distilled water as a negative control [17]. The inhibition zones (ZOI) were measured after 24 h of incubation at 37 °C. Moderate activity was shown by ZnO nanoparticles displaying ZOI 13.6 mm and 14.2 mm for E. coli and S. aureus, respectively.

In contrast, Ni-doped ZnO not only exhibited much-promoted activities with the ZOI as 18.1 mm for E. coli and 19.0 mm for S. aureus. Inhibition zones were not observed for distilled water, confirming that only nanoparticles contributed to the antimicrobial activity. Compared toure ZnO, the wider inhibition zones indicate more potent activity of Ni-doped ZnO against both Gram-positive and Gram-negative bacteria [18].

Mechanisms of Antimicrobial Action

The improved antibacterial efficiency of Ni-doped ZnO can be ascribed to the generation of reactive oxygen species (ROS) such as hydroxyl radical (•OH), superoxide radical O_2^{-}• and hydrogen peroxide (H_2O_2). ROS causes oxidative stress, leading to lipid peroxidation, protein denaturation, and DNA damage to bacteria. The surface defect density of a semiconductor induces more active sites for ROS generation, while ni doping quenches oxygen radicals at the surface of semiconductors, which also enhances the interaction of ni with bacterial membranes [19]. These positively charged nanoparticles provide electrostatic interactions that destroy the membrane integrity of the negatively charged bacteria, leading to leakage of intracellular contents and death of bacterial cells [20].

Effectiveness of Ni Doping in Enhancing Antimicrobial Properties

The effect of Ni doping on ZnO nanoparticle antimicrobial efficacy is by conducting bandgap analysis, which shows that the bioactivity of ZnO nanoparticles improves with the decrease of bandgap, leading to increased production of reactive oxygen species (ROS), and bioactivity by releasing Zn^{2+} and Ni^{2+} ions that interrupt bacterial enzyme function. ROS generation, membrane integrity disruption, and ion toxicity thus became MAGIC, making Ni-doped ZnO billion-fold less effective than pristine ZnO. This suggests its possible use in applications such as antimicrobial coatings, water disinfection and healthcare [21].

Table 1: Antimicrobial Activity of ZnO and Ni-doped ZnO Nanoparticles

Sample	Zone of Inhibition (ZOI) in mm	
	E. coli (Gram-negative)	S. aureus (Gram-positive)
ZnO	13.6 ± 0.4	14.2 ± 0.3
Ni-doped ZnO	18.1 ± 0.5	19.0 ± 0.6

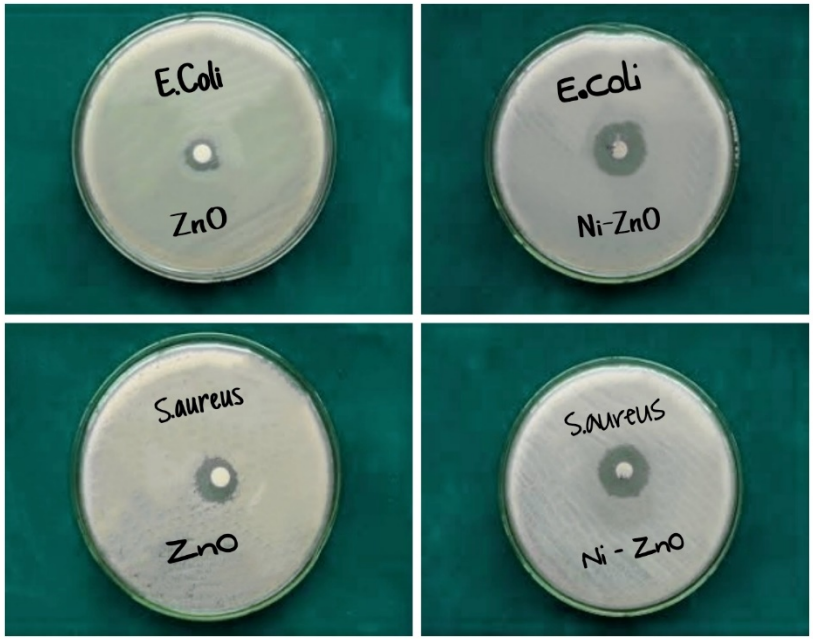

Figure 6. Zone of Inhibition for ZnO and Ni-doped ZnO NPs Against E. coli and S. aureus

Conclusion

In this study, we have successfully synthesized and characterized both pristine and Ni-doped ZnO nanoparticles and established the vital role of Ni doping on various properties such as structural, optical and antimicrobial. Upon Ni doping, although the crystallite size increased, the hexagonal wurtzite structure was confirmed to be retained, according to XRD. Optical examinations showed bandgap narrowing from 2.9 eV to 2.6 eV, improving visible light absorption. The Ni-doped ZnO showed more efficient antimicrobial properties with higher inhibition zone diameters than the ZnO against Escherichia coli and Staphylococcus aureus. This enhanced activity is due to more generation of reactive oxygen species (ROS), enhanced bacterial membrane disturbance, and more Zn^{2+} and Ni^{2+} ions release. The study showcases the untapped potential of Dopant: Ni as a multifunctional material for antimicrobial applicability, water purification technology, and optoelectronics realization. The discoveries will enable next-generation nanomaterials for specific environmental and healthcare applications.

References

[1] Y. Zaman *et al.*, "Modified physical properties of Ni doped ZnO NPs as potential photocatalyst and antibacterial agents," *Arabian Journal of Chemistry*, vol. 16, no. 11, 2023, doi: 10.1016/j.arabjc.2023.105230.

[2] S. R. Patel *et al.*, "Pristine, Ni- and Zn-Doped CuSe Nanoparticles: An Antimicrobial, Antioxidant, and Cytotoxicity Study," *ACS Appl Bio Mater*, vol. 6, no. 6, 2023, doi: 10.1021/acsabm.3c00090.

[3] K. L. Mary, J. V. Manonmoni, A. M. R. Balan, P. S. Karthik, and S. P. Malliappan, "Phytochemical assisted synthesis of Ni doped ZnO nanoparticles using aloe vera extract for enhanced photocatalytic and antibacterial activities," *Dig J Nanomater Biostruct*, vol. 17, no. 2, 2022, doi: 10.15251/DJNB.2022.172.634.

[4] M. A. Qamar, M. Javed, and S. Shahid, "Designing and investigation of enhanced photocatalytic and antibacterial

properties of 3d (Fe, Co, Ni, Mn and Cr) metal-doped zinc oxide nanoparticles," *Opt Mater (Amst)*, vol. 126, 2022, doi: 10.1016/j.optmat.2022.112211.

[5] M. A. Qamar *et al.*, "Designing of highly active g-C3N4/Ni-ZnO photocatalyst nanocomposite for the disinfection and degradation of the organic dye under sunlight radiations," *Colloids Surf A Physicochem Eng Asp*, vol. 614, 2021, doi: 10.1016/j.colsurfa.2021.126176.

[6] A. Mohan *et al.*, "Nanostructured nickel doped zinc oxide material suitable for magnetic, supercapacitor applications and theoretical investigation," *Chemosphere*, vol. 299, 2022, doi: 10.1016/j.chemosphere.2022.134366.

[7] N. Shanmugam *et al.*, "Influence of Cerium and Nickel Co-Doping on ZnO Nanostructures for Electrochemical Behavior of H2O2 Sensing Applications," *Sustainability (Switzerland)*, vol. 14, no. 10, 2022, doi: 10.3390/su14106353.

[8] I. Ngom, N. M. Ndiayea, A. F. M. Bakayoko, B. D. Ngom, and M. Maaza, "On the Use of Moringa Oleifera Leaves Extract for the Biosynthesis of NiO and ZnO Nanoparticles," *MRS Adv*, vol. 5, no. 21–22, 2020, doi: 10.1557/adv.2020.212.

[9] N. Goswami and A. Sahai, "Structural transformation in nickel doped zinc oxide nanostructures," *Mater Res Bull*, vol. 48, no. 2, 2013, doi: 10.1016/j.materresbull.2012.10.045.

[10] A. Doria-Manzur, H. Sharifan, and L. Tejeda-Benitez, "Application of zinc oxide nanoparticles to promote remediation of nickel by Sorghum bicolor: metal ecotoxic potency and plant response," *Int J Phytoremediation*, vol. 25, no. 1, 2023, doi: 10.1080/15226514.2022.2060934.

[11] M. Ali *et al.*, "Preparation of Co and Ni doped ZnO nanoparticles served as encouraging nano-catalytic application," *Mater Res Express*, vol. 6, no. 12, 2019, doi: 10.1088/2053-1591/ab6383.

[12] A. C. Nwanya, S. Botha, F. I. Ezema, and M. Maaza, "Functional metal oxides synthesized using natural extracts from waste maize materials," *Current Research in Green and Sustainable Chemistry*, vol. 4, 2021, doi: 10.1016/j.crgsc.2021.100054.

[13] F. Islam *et al.*, "Exploring the Journey of Zinc Oxide Nanoparticles (ZnO-NPs) toward Biomedical Applications," 2022. doi: 10.3390/ma15062160.

[14] G. Faye, T. Jebessa, and T. Wubalem, "Biosynthesis, characterisation and antimicrobial activity of zinc oxide and nickel doped zinc oxide nanoparticles using Euphorbia abyssinica bark extract," *IET Nanobiotechnol*, vol. 16, no. 1, 2022, doi: 10.1049/nbt2.12072.

[15] M. Hessien, E. Da'na, and A. Taha, "Phytoextract assisted hydrothermal synthesis of ZnO–NiO nanocomposites using neem leaves extract," *Ceram Int*, vol. 47, no. 1, 2021, doi: 10.1016/j.ceramint.2020.08.192.

[16] P. Gnanamozhi *et al.*, "Influence of Nickel concentration on the photocatalytic dye degradation (methylene blue and reactive red 120) and antibacterial activity of ZnO nanoparticles," *Ceram Int*, vol. 46, no. 11, 2020, doi: 10.1016/j.ceramint.2020.05.054.

[17] N. S. Mohan, S. Bhuvaneswari, R. Anitha, and V. Vijayalakshmi, "Improved photocatalytic degradation of organic pollutants using green synthesized ZnO and Ni@ZnO NPs for environmental applications," *Environ Nanotechnol Monit Manag*, vol. 21, 2024, doi: 10.1016/j.enmm.2024.100922.

[18] M. Ashokkumar and C. Muthusamy, "Role of ionic radii and electronegativity of co-dopants (Co, Ni and Cr) on properties of Cu doped ZnO and evaluation of In-vitro cytotoxicity," *Surfaces and Interfaces*, vol. 30, 2022, doi: 10.1016/j.surfin.2022.101968.

[19] P. S. Vindhya, R. Kunjikannan, and V. T. Kavitha, "Bio-fabrication of Ni doped ZnO nanoparticles using Annona Muricata leaf extract and investigations of their antimicrobial, antioxidant and photocatalytic activities," *Phys Scr*, vol. 98, no. 1, 2023, doi: 10.1088/1402-4896/acaa10.

[20] S. Naseer *et al.*, "Synthesis of Ni-Ag-ZnO solid solution nanoparticles for photoreduction and antimicrobial applications," *RSC Adv*, vol. 12, no. 13, 2022, doi: 10.1039/d2ra00717g.

[21] H. H. Kim, W. Han, K. H. An, and B. J. Kim, "Preparation of nickel coated-carbon nanotube/zinc oxide nanocomposites and their antimicrobial and mechanical properties," *Applied Chemistry for Engineering*, vol. 27, no. 5, 2016, doi: 10.14478/ace.2016.1071.